# X-ray Crystal Structures and Photophysical Properties of New Conjugated Oligoquinolines

Ashok S. Shetty,[†] Elizabeth B. Liu,[†]
Rene J. Lachicotte,[‡] and Samson A. Jenekhe*[,†,‡]

*Departments of Chemical Engineering and Chemistry and Center for Photoinduced Charge Transfer, University of Rochester, Rochester, New York 14627-0166*

*Received December 11, 1998*
*Revised Manuscript Received July 14, 1999*

The synthesis, electronic structure, and optical, nonlinear optical and charge transport properties of numerous conjugated oligomers[1a] of polyenes,[1b] acenes,[1b] thiophene,[1c] pyrrole,[1d] *p*-phenylene,[1b] and *p*-phenylenevinylene[1a,2] have been extensively investigated both as p-type (hole transport) organic semiconductors per se and as structurally well-defined model systems for the corresponding conjugated polymers.[1a] Few, if any, oligomers of n-type (electron transport) conjugated polymers such as the polyquinolines[3−9] are known. We report herein the synthesis, single-crystal X-ray structures, and the photophysical properties of two new conjugated oligoquinolines. The oligomers are promising model systems for elucidating the structure−property relationships of conjugated polyquinolines and may also be useful as n-type semiconductors for device applications.

The n-type conjugated polymers by virtue of their electron transport, high electron affinity and interesting photophysical properties are of growing interest in electronic and optoelectronic devices. Polyquinolines, in particular, with the general structure **1** (Scheme 1) are high temperature (glass transitions above 200 °C and decomposition temperatures above 500 °C) conjugated polymers and possess interesting mechanical,[3] photoresponsive and photoconductive,[4] electron transport,[5−7] third-order nonlinear optical,[8] and electroluminescent[6,7] properties. They have thus been attracting considerable attention for their potential use in thin film electronic and optoelectronic devices.[6,7]

Although over several dozen polyquinolines have been reported in the last two decades,[3−9] only one preliminary report has discussed the crystal structure of a rigid-rod polyquinoline, poly[2,2′-(*p*,*p*′-biphenylene)-6,6-bis(4-phenylquinoline)] (**1b**, PBPQ).[9] The study concluded that X-ray diffraction pattern of fibers spun from anisotropic solutions of this polymer showed that parallel chains along the direction of the fiber axis stack in nearly coplanar sheets with the two pendant phenyl groups on the 4-position of the quinoline units pointing toward one another.[9] The close packing of the polymer chains was invoked to explain the poor solubility in aprotic organic solvents and the photophysical properties[4−8] of the polyquinolines. However, a more rigorous study of the crystal structure of the conjugated polyquinolines by using monodisperse oligomers as model systems has not been conducted.

We synthesized and characterized 2,2′-bis(4-phenylquinoline)-1,4-phenylene (**2a**) and 2,2′-bis(4-phenylquinoline)-4,4′-biphenylene (**2b**) and obtained single-crystal X-ray structures for and investigated the photophysical properties of these compounds (Scheme 1). Oligoquinolines **2a** and **2b** were synthesized by the Friedlander coupling[10] of 2 equiv of 2-aminobenzophenone with 1 equiv of 1,4-diacetylbenzene or 4,4′-diacetylbiphenylene, respectively.[11]

Single crystals of the oligomers suitable for X-ray structural determination were obtained from concentrated chloroform solutions (30 mg/mL). Whereas **2a** crystallized as clusters of needles, **2b** crystallized as clusters of overlapping irregularly shaped blocks. Laue symmetry revealed a monoclinic crystal system for both

[†] Department of Chemical Engineering and Center for Photoinduced Charge Transfer.

[‡] Department of Chemistry.

(1) See the comprehensive recent reviews on diverse p-type conjugated oligomers: (a) Müllen, K., Wegner, G., Eds. *Electronic Materials: The Oligomer Approach*; Wiley-VCH: Weinheim, Germany, 1998. (b) Geerts, Y.; Klärner, G.; Müllen, K. In *Electronic Materials: The Oligomer Approach*; Müllen, K., Wegner, G., Eds.; Wiley-VCH: Weinheim, Germany, 1998; pp 1−103. (c) Baüerle, P. In *Electronic Materials: The Oligomer Approach*; Müllen, K., Wegner, G., Eds.; Wiley-VCH: Weinheim, Germany, 1998; pp 105−197. (d) Groenedaal, L.; Meijer, E.-W.; Vekemans, J. A. J. M. In *Electronic Materials: The Oligomer Approach*; Müllen, K., Wegner, G., Eds.; Wiley-VCH: Weinheim, Germany, 1998; pp 235−272.

(2) (a) Drefahl, G.; Plötner, G. *Chem. Ber.* **1961**, *94*, 907−914. (b) For a more recent study see: Gill, R. E.; Meetsma, A.; Hadziioannou, G. *Adv. Mater.* **1996**, *8*, 212−214.

(3) (a) Sybert, P. D.; Beever, W. H.; Stille, J. K. *Macromolecules* **1981**, *14*, 493−502. (b) Pelter, M. W.; Stille, J. K. *Macromolecules* **1990**, *23*, 2418−2422.

(4) (a) Zimmerman, E. K.; Stille, J. K. *Macromolecules* **1985**, *18*, 321−327. (b) Abkowitz, M. A.; Stolka, M.; Antoniadis, H.; Agrawal, A. K.; Jenekhe, S. A. *Solid State Commun.* **1992**, *83*, 937−941.

(5) (a) Agrawal, A. K.; Jenekhe, S. A. *Chem. Mater.* **1992**, *4*, 95−104. (b) Agrawal, A. K.; Jenekhe, S. A. *Macromolecules* **1993**, *26*, 895−905. (c) Agrawal, A. K.; Jenekhe, S. A. *Chem. Mater.* **1996**, *8*, 579−589. (d) Agrawal. A. K.; Jenekhe, S. A. *Chem. Mater.* **1993**, *5*, 633−640.

(6) Zhang, X.; Shetty, A. S.; Jenekhe, S. A. *Acta Polym.* **1998**, *49*, 52−55.

(7) (a) Jenekhe, S. A.; Zhang, X.; Chen, X. L.; Choong, V.-E.; Gao, Y.; Hsieh, B. R. *Chem. Mater.* **1997**, *9*, 409−412. (b) Zhang, X.; Shetty, A. S.; Jenekhe, S. A. *SPIE Proc.* **1997**, *3148*, 89−101.

(8) Agrawal, A. K.; Jenekhe, S. A.; Vanherzeele, H.; Meth, J. S. *J. Phys. Chem.* **1992**, *96*, 2837−2843.

(9) (a) Sutherlin, D. M.; Stille, J. K. *Macromolecules* **1985**, *18*, 2669−2675. (b) Burkhart, C. W.; Lando, J. B.; Stille, J. K. *Mater. Res. Soc. Symp. Proc.* **1989**, *134*, 475−483.

(10) Friedlander, P. *Ber. Dtsch. Chem. Ges.* **1882**, *16*, 2572−2575.

(11) 2-Aminobenzophenone, 1,4-diacetylbenzene, 4,4′-diacetylbiphenyl, and diphenyl phosphate (Aldrich) were used without further purification. The synthetic procedure involved stirring a solution of 2-aminobenzophenone (18.5 mmol), diketone (6.16 mmol), and diphenyl phosphate (123 mmol) in freshly distilled *m*-cresol (3 mL) in a sealed tube at 140 °C under an argon atmosphere. The excess amount of 2-aminobenzophenone ensured that all the diacetyl groups in a diketone were reacted. After 6 h, the solution was cooled and poured into a solution of 10% triethylamine in methanol (300 mL) and the crude product was collected by filtration. The oligomers were purified by recrystallization from a 1: 4 mixture of tetrahydrofuran and methanol. **2,2′-Bis(4-phenylquinoline)-1,4-phenylene (2a)** (3.23 g, 98%). Mp: 251−252 °C. MS (EI): 484 (calculated for $C_{36}H_{24}N_2$), 484 (found). $R_f$ (hexane:THF, 9:1): 0.4. $^1$H NMR (300 MHz, $CDCl_3$): $\delta$ 8.52 (s, 4H), $\delta$ 8.31 (d, 2H), $\delta$ 7.97 (d, 2H), $\delta$ 7.94 (s, 2H), $\delta$ 7.78 (s, 2H), $\delta$ 7.6 (m, 12H).$^{13}$C NMR (400 MHz, $CDCl_3$): $\delta$ 156.22, 149.3, 148.8, 138.4, 130.2, 129.6, 128.6, 128.5, 128.1, 128.0, 126.5, 125.9, 125.7, 119.4, 119.3. **2,2′-bis(4-phenylquinoline)-4,4′-biphenylene (2b)** (1.5 g, 98%). Mp: 252−253 °C. MS (EI): 560 (calculated for $C_{42}H_{28}N_2$), 560 (found): $R_f$ (hexane:THF, 6:1): 0.49. $^1$H NMR (300 MHz, $CDCl_3$): $\delta$ 8.36 (d, 4H), $\delta$ 8.31 (d, 2H), $\delta$ 7.95 (d, 2H), $\delta$ 7.90 (s, 2H), $\delta$ 7.85 (d, 4H), $\delta$ 7.78 (t, 2H), $\delta$ 7.55 (m, 12H) $\delta$ 7.50 (t, 2H).$^{13}$C NMR (400 MHz, $CDCl_3$): 156.3, 149.2, 148.9, 141.4, 138.8, 138.4, 130.2, 129.6, 128.6, 128.4, 128.0, 127.5, 126.4, 125.8, 125.7, 119.3, 119.2.

10.1021/cm981121p CCC: $18.00 
Published on Web 08/17/1999

**Scheme 1**

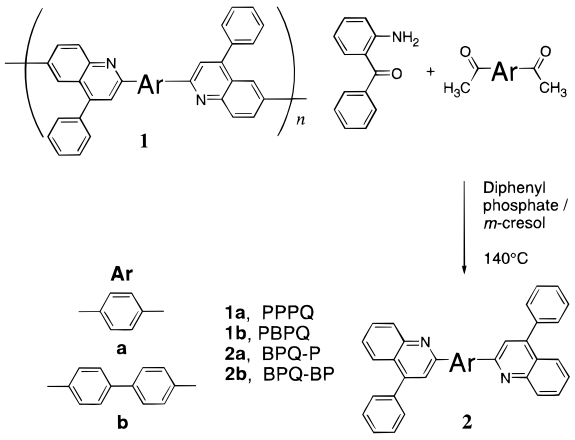


**2a** and **2b**. The unit cell parameters of $a = 13.9932(8)$ Å, $b = 4.0104(2)$ Å, $c = 21.6130(13)$ Å, and $\beta = 96.0320(10)$ for **2a** and of $a = 11.4460(2)$ Å, $b = 8.3789(2)$ Å, $c = 15.8601(3)$ Å, and $\beta = 105.9710(10)$ for **2b** were based upon the least-squares refinement of three-dimensional centroids of >3000 reflections for each crystal. The space groups were assigned as $P2/c$ and $P2_1/c$, respectively for **2a** and **2b**, and the structures refined to final residuals of $R_1 = 3.95\%$ for **2a**, and $R_1 = 4.52\%$ for **2b**. Further experimental details of the data collection and structure refinement can be found in the Supporting Information.

The molecular structure and crystal packing of the two oligomers are shown in Figures 1 and 2, respectively. In the crystal of oligomer **2a**, the molecule is located on a crystallographic center of symmetry at the midpoint of the central *p*-phenylene ring. The molecule in the crystal of oligomer **2b** is located on a crystallographic center of symmetry at the midpoint of the central inter-ring bond. In both oligomers, the quinoline moieties are in a crystallographically imposed *anti*-orientation with respect to each other. This result is very different from the *syn*-conformation of **1b** proposed from X-ray diffration patterns of fibers.[9] However, because the prior crystal structure of **1b** was based on few unique reflections in the fiber diffraction and untested assumptions in the molecular packing modeling,[9] the *anti*-conformation of the chain structures of polyquinolines **1a** and **1b,** which is suggested from the presented single-crystal structures of oligoquinolines **2a** and **2b**, is to be taken as the more definitive structure. The central *p*-phenylene ring in **2a** is twisted 26° from the mean plane of the quinoline moieties. Although the central phenylenes in oligomer **2b** are coplanar, they are twisted 13° relative to the mean plane of the quinoline moieties. The phenyl groups appended onto the quinoline moieties in both oligomers are twisted ca. 49° relative to the quinoline moieties.

The molecular packing of the oligomers, as shown in Figures 1C and 2C, are dramatically different. In the case of **2a** (Figure 1C), the molecules pack in columns exhibiting intermolecular *face-to-face* $\pi$ stacking (sandwich-type) separated by ca. 4 Å.[12] The pendant phenyl groups pack in a way that precludes intercolumn $\pi$-stacking. Oligomer **2b** (Figure 2C), packs is a more

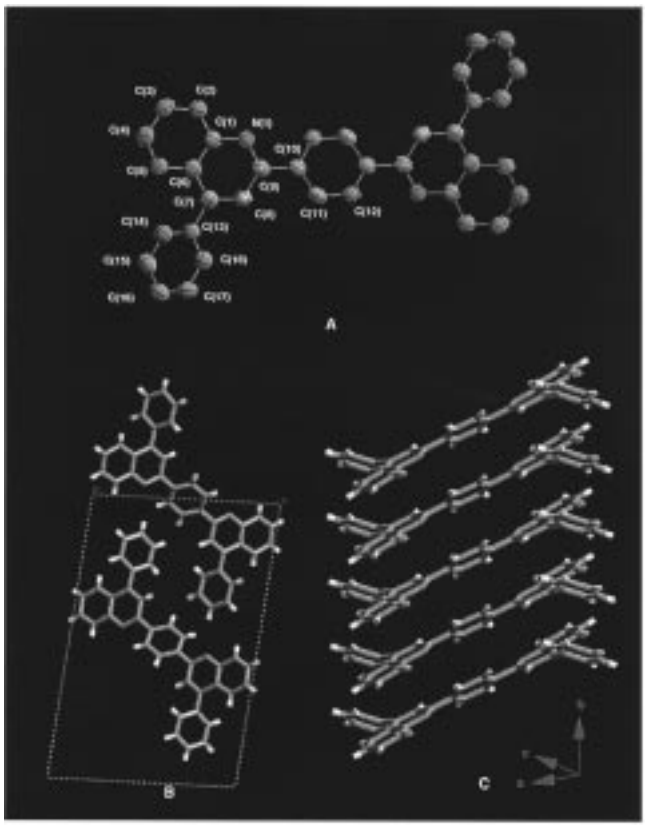


**Figure 1.** (A) 30% ORTEP diagram of oligomer **2a** with the atom numbering scheme. Because the molecule has an inversion center at the midpoint of the central phenylene ring, the symmetry related atoms are not labeled. (B) Organization of the molecules in a single unit cell. (C) Packing of the molecules along the *b*-axis with intermolecular distance of 4 Å.

complex fashion. It is dominated by an intermolecular *edge-to-face* packing between the pendant phenyl and the biphenylene rings and between the pendant phenyl and the quinoline moieties at an intermolecular distance of ca. 3.6 Å. Careful examination of the crystal structure reveals that the pendant phenyl groups are engaged in $\pi-\pi$ interactions with both the biphenylene and the quinoline moieties of **2b**.

Optical absorption and fluorescence spectra of **2a** and **2b** in solution (chloroform and formic acid) are shown in Figure 3. The absorption maxima of **2b**, with a biphenylene linkage, is red shifted from that of **2a** in both solvents (Figure 3). The absorption spectrum of **2a** in chloroform (Figure 3A) shows peaks at 280 and 342 nm whereas that of **2b** reveals peaks at 294 and 348 nm. In the case of **2a**, the lower energy band is only 60% in intensity of the peak at 280 nm. In the case of **2b**, however, the two absorption bands are nearly of comparable intensity. When the solvent is changed to formic acid, in which the quinoline moieties are protonated, the absorption spectra of these oligomers change significantly (Figure 3 B). For oligomer **2a**, the absorption peak is red shifted by 20 nm as compared to that in chloroform (from 342 to 362 nm) whereas **2b** exhibits a much larger red shift of 32 nm in absorption $\lambda_{max}$ (from 348 to 380 nm).

The emission spectra of the oligoquinolines show similar dependences on the size of the aromatic group that links the two quinoline moieties and the solvent environment. The emission spectrum of **2b** in chloroform

(12) (a) Williams, J. H. *Acc. Chem. Res.* **1993**, *26*, 593−598. (b) Desiraju, G. R.; Gavezzotti, A. *J. Chem. Soc., Chem. Commun.* **1989**, 621−623.

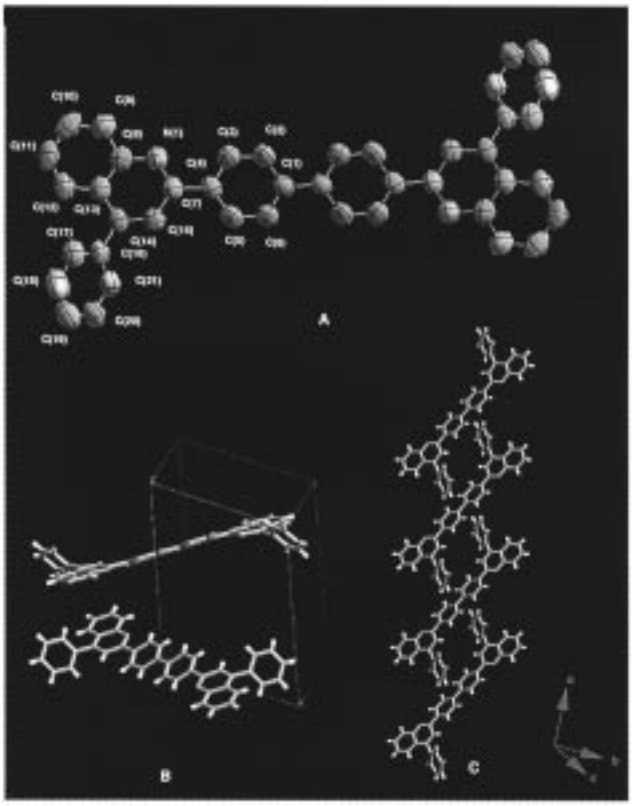


**Figure 2.** (A) 30% ORTEP diagram of oligomer **2b** with the atom numbering scheme. Because the molecule has an inversion center at the midpoint of the central C−C bond, the symmetry related atoms are not labeled. (B) Organization of the molecules in a single unit cell. (C) Packing of the molecule, with an intermolecular distance of 3.6 Å. Note the edge-to-face packing between the pendant phenyl groups and the biphenylene moieties in part C.

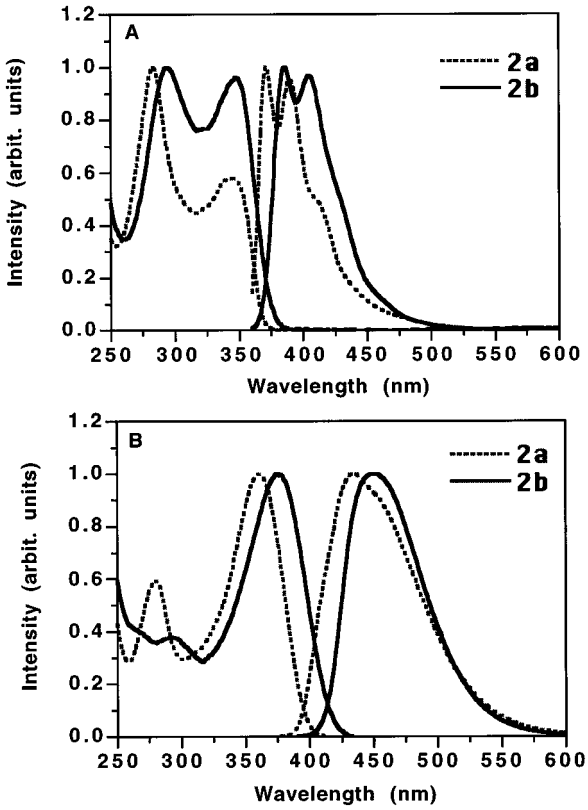


**Figure 3.** Optical absorption and fluorescence spectra of oligomers **2a** (dashed lines) and **2b** (solid lines) in (A) chloroform ($2 \times 10^{-5}$ M) and (B) formic acid ($2 \times 10^{-5}$ M).

(Figure 3A) is red shifted from the emission maxima of **2a** (370 nm) by 14 nm. A similar red shift of 14 nm was observed between the emission maxima of **2a** (436 nm) and **2b** (450 nm) in formic acid (Figure 3B). The emission maxima of both **2a** and **2b**, in formic acid, are red shifted by 66 nm compared to those in chloroform. In addition, as can be seen in parts A and B of Figure 3, the emission bands of both oligomers in formic acid are broader and less structured than those in chloroform. The luminescence quantum yields ($\Phi$)[13] of **2a** were 7 and 41% in chloroform and formic acid, respectively, whereas **2b** had a $\Phi$ of 54% in both solvents. Thus, oligomer **2a** has a higher luminescence quantum efficiency in formic acid than in chloroform whereas in the same solvent systems **2b** is much more fluorescent than **2a**.

The bathochromic shift of the optical absorption of **2b** compared to **2a** is due in part to the larger number of $\pi$-electrons and a greater degree of $\pi$-electron delocalization along the oligomer backbone. The observed photophysical properties also suggest the presence of intramolecular charge transfer (ICT) between the central phenylene rings as donor groups and the quinoline moieties as acceptors.[14] The ICT is greater in **2b** than in **2a** because the biphenylene moiety is a stronger $\pi$-electron donor than the single phenylene group in **2a**. In formic acid, protonation of the quinoline moieties makes them stronger acceptors, thereby enhancing the ICT, which accounts for the large spectral red shifts compared to chloroform. These oligomer results confirm that the previously reported effects of protonation on electronic delocalization of the conjugated polyquinolines are intrinsic to their molecular structures (repeat units).[5]

Optical absorption and fluorescence spectra of thin films of **2a** and **2b**, spin cast onto fused silica substrates from chloroform solutions, were also measured. The absorption spectrum of **2a** shows peaks at 284 and 346 nm whereas that of **2b** reveals peaks at 296 and 352 nm (Figure 4). The greater degree of $\pi$-electron delocalization of **2b** is in accord with the crystal structures of oligomer **2b**. As discussed above, the central aromatic rings in oligomer **2b** (Figure 2A) are mutually coplanar and are twisted 13° from the quinoline moieties whereas the phenylene ring in **2a** is twisted 26° (Figure 1A) from the quinoline moieties, reducing efficient $\pi$-electron delocalization. The solid-state absorption spectra of **2a** and **2b** are also very similar to the dilute chloroform solution results, suggesting that aggregation of oligomer molecules does not significantly modify the electronic ground state of the materials.

Freshly cast films of both oligomers had a broad emission maxima at 420 nm. After 24 h under ambient

(13) Instruments and procedures for the characterization of the solution and solid-state absorption spectra, emission spectra, and fluorescence quantum yield are identical to those described by us previously: (a) Osaheni, J. A.; Jenekhe, S. A. *J. Am. Chem. Soc.* **1995**, *117*, 7389−7398. (b) Osaheni, J. A.; Jenekhe, S. A. *Macromolecules* **1994**, *27*, 739−742.

(14) Slama-Schwok, A.; Blanchard-Desce, M.; Lehn, J.-M. *J. Phys. Chem.* **1990**, *94*, 3894−3902.

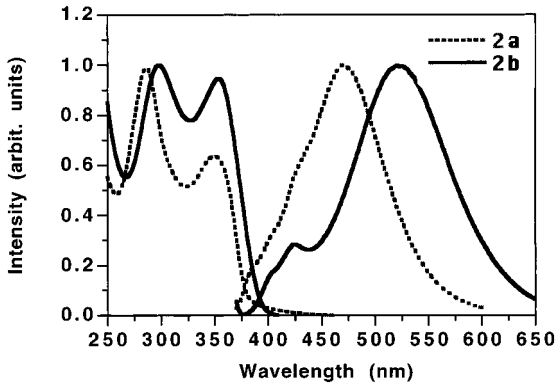


**Figure 4.** Absorption and emission spectra of spin coated thin films of oligomers **2a** (dashed lines) and **2b** (solid lines) on fused silica substrates after annealing at 70 °C.

conditions, the **2a** film exhibited an emission maxima at 470 nm whereas the **2b** film still showed one emission peak at 420 nm with a shoulder at ca.. 470 nm. However when the films were annealed at 70 °C in a vacuum oven for 24 h, the **2b** film exhibited an emission maxima at 515 nm, whereas the emission maxima of the **2a** film remained unchanged at 470 nm (Figure 4). Because the thin film annealing process for **2b** takes longer compared to that of **2a**, it may be implied that the packing mode of **2b** in the solid state is more complicated than that of **2a** as confirmed by the single-crystal X-ray structures of these oligomers. Annealed films of **2a** and **2b** had estimated fluorescence quantum yields[13] of 20% and 43%, respectively, which are consistent with the results in solution. The **2a** and **2b** emission bands at 470 and 515 nm, respectively, are significantly red shifted (100−131 nm) from their corresponding emission spectra in dilute chloroform solution. The strong $\pi-\pi$ stacking interactions evident in the X-ray crystal structures of these oligomers clearly influence their excited-state electronic structures. However, although excimer formation[15] is the likely explanation of the solid state emission spectra, additional studies are needed to confirm this particularly in oligomer **2b**.

In summary, two new conjugated oligoquinolines, **2a** and **2b**, have been synthesized and their molecular and photophysical properties were characterized. The single-crystal X-ray structures of these oligomers provide the first detailed structural information on the numerous polyquinolines.[3−9] Both **2a** and **2b** crystallized in a monoclinic lattice with different unit cell parameters and space groups. The X-ray crystal structures reveal that **2a** exhibits intermolecular face-to-face $\pi-\pi$ stacking whereas **2b** manifests edge-to-face packing. The dilute solution and solid-state optical absorption and emission spectra of **2b** were red shifted from those of **2a** because of the greater degrees of $\pi$-electron delocalization and intramolecular charge transfer in **2b** compared to **2a**. The strongly Stokes shifted solid-state emission bands of both oligomers are attributed to excimer formation. These conjugated oligoquinolines with known X-ray crystal structures are excellent model systems for elucidating the structures and properties of polyquinolines and may also find device applications as n-type semiconductors.

**Acknowledgment.** This research was supported by the Office of Naval Research and in part by the National Science Foundation (CTS-9311741).

**Supporting Information Available:** Text giving synthetic procedures and characterization of **2a** and **2b**, figures showing $^1$H NMR spectra of **2a** and **2b**, text giving experimental details for the X-ray crystallography, and tables of atomic coordinates, bond lengths and angles, anisotropic displacement parameters, and hydrogen atom coordinates. This material is available free of charge via the Internet at http://pubs.acs.org.

CM981121P

(15) Jenekhe, S. A.; Osaheni, J. A. *Science* **1994**, *265*, 765−768.